https://doi.org/10.1016/j.apenergy.2018.01.099 **This is the Pre-Published Version.**

Integrated energy performance optimization of a passively designed high-rise residential building in different climatic zones of China

Xi Chen* and Hongxing Yang

Renewable Energy Research Group (RERG), Department of Building Services Engineering, The Hong Kong Polytechnic University, Kowloon, Hong Kong, China

Abstract

This paper mainly focuses on investigating the influence of weather conditions on the sensitivity analysis and optimization of a typical passively designed high-rise residential building. A holistic passive design approach combining a variance-based factor prioritizing and surrogate model based multi-objective optimization was previously proposed to explore the green building solution in the hot and humid climate of Hong Kong. The design approach is further extended for application into a broader spectrum of climates across the mainland of China, including the severe cold zone, cold zone, hot summer cold winter zone, temperate zone as well as hot summer warm winter zone. The relative weight analysis is first compared with the Fourier Amplitude Transformation Analysis (FAST) in prioritizing the weighting of design inputs for different climatic zones. The relative weight analysis is then proved a feasible alternative sensitivity analysis method when its corresponding multiple linear regression (MLR) model can achieve good prediction performance. Furthermore, a tuning program in R is developed to improve the prediction performance of surrogate models with the Support Vector Machine (SVM) algorithm under above climatic zones. The model fitting performance with SVM is proved to be greatly improved by modifying the Sigma and C parameters. Finally, optimum design options under the five climatic zones are discussed in relation to the outdoor thermal, ventilation and solar radiation conditions. This research explored the applicability of the proposed passive design optimization approach in diverse climates, and can therefore prompt decision-makers' endorsement as a national green building design tool in the early planning stage.

Keywords: Surrogate model; Weather conditions; Passive design; Sensitivity analysis; Optimization

1. Introduction

* Corresponding author: Tel.:+852-2766 4726, Fax: 2765 7198, E-mail: climber027@gmail.com

Buildings account for more than 40% of the global energy consumption, and the residential energy use in China ranks first in main countries of the world [1]. High-rise residential buildings with prefabricated standard units are becoming a popular construction practice in densely populated areas to increase the land use efficiency [2]. Passive design strategies, recommended as alternative energy reduction approaches in many green building guidelines (e.g. LEED, BEAM, BREEAM), are attracting more attention in building industries because of their potential in maintaining quality indoor environment and reducing energy demands [3, 4]. However, some passive strategies such as the ground cooling and green roof have constrained applicability in high-rise buildings owing to roof area, site coverage and structural load limitations. Previous studies conducted by the authors have identified important passive architectural design parameters covering the building layout, envelop thermophysics, building geometry and infiltration & air-tightness based on their contributions to indoor thermal, ventilation and daylight performances [5-7]. Prioritized design features from sensitivities analyses were further coupled with the Non-dominated Sorting Genetic Algorithm-II (NSGA-II) to explore the optimal building design based on the developed surrogate models from robust statistical modelling experiments [8]. These previous works mainly applied passive architectural designs to the hot and humid climate of Hong Kong, where the hybrid ventilation is controlled by the adaptive comfort model (ACM) to minimize the operation of HVAC systems [9]. To explore the applicability of the proposed holistic design optimization approach in more diverse meteorological conditions, suitable ACMs for different areas have to be derived from field tests and statistical analyses.

The ASHRAE 55% adaptive comfort model is developed to address the psychological shift and acclimation of building occupants in a specified range of the outdoor temperature, air speed, metabolic rate [10]. It is originally designed for the indoor comfort assessment in natural ventilation conditions [11, 12], while has been extended to mixed-model buildings where natural ventilation is supplemented with necessary mechanical cooling [13, 14]. The cooling system is controlled to maintain the indoor operative temperature between the upper and lower acceptable limits of the ASHRAE 55 ACM. Such an extended application of ACMs is only considered appropriate when the indoor environmental control is completely subject to occupants such as in a residential building. Apart from optimizing building energy use in the hot and humid climate, the ASHRAE 55 ACM is

also used for summer time building performance evaluation, whenever the prevailing mean outdoor temperature is within model requirements [15-17]. Similar to the approach from which the ASHRAE 55 ACM was derived, Yan et al. built adaptive comfort models for four climatic zones of China. Indoor neutral temperatures were expressed by linear regression equations, whose prediction accuracy could compete with current international models such as ASHRAE 55 and EN 15251 within their required outdoor temperature ranges [18]. This study, however, did not give out the acceptable comfort limits which are necessary for typical air-conditioning controllers. A more detailed study was then carried out in the cold Tibet area of China, where acceptable operative temperature ranges were obtained for difference indoor humidity levels [19]. Indoor temperature limits of 90% acceptability for the same area were also derived from a second-order polynomial equation, which could be used to formulate an ACM model in the cold area [20]. In moderate climates, where winter outdoor conditions are between the cold and hot areas, the ASHRAE 55 ACM model was adopted to address summer time thermal comfort, while a modified linear equation was proposed when the prevailing mean outdoor temperature is lower than 12 ℃ [21]. Sourbron and Helsen also proposed an ACM for moderate climates, where comfort limits kept constant as the mean outdoor temperature dropped below 10 ℃ [22]. Above ACMs are widely used in temperature settings or comfort assessments in building energy studies to explore the extent to which the operation of active building systems can be avoided [23, 24].

From the above introduction and literature review, it can found out that applying integrated sensitivity analysis and optimization to passively designed high-rise residential buildings in diversified climatic conditions are seldom addressed by existing research. Most studies focus on one specific climate which are limited by certain external conditions or design options. Optimized passive design solutions are also scarcely related to detailed weather parameters. Furthermore, surrogate models developed for design optimizations are not sufficiently tuned to improve the prediction performance according to the best knowledge of authors. To fill these research gaps, this paper comprehensively investigates the influence of climatic conditions on the proposed holistic design optimization approach within the broad area of mainland China. The parameter setting of statistical models is optimized for the application in different climatic zones. In addition, a prospective alternative sensitivity analysis method to the variance-based approach is explored by comparative

modelling experiments.

2. Research design and methodology

Both the sensitivity analysis and design optimization of the passively designed prototype building are subject to variation of weather conditions in this research according to Fig. 1. A dynamic hybrid ventilation control algorithm is applied to the developed generic model in EnergyPlus to calculate building energy demands based on randomly generated design inputs. The relative weight analysis is compared with the FAST method by deriving sensitivity indices for different climatic regions. The uncertainty of sensitivity indices is also estimated by bootstrapping to pick out the most important design parameters for each region. On the other side, the Support Vector Machine (SVM) is used to train the surrogate model based on sampled design inputs and simulated energy demand outputs. The surrogate model is then refined by a multi-criterion tuning program in R to obtain the optimal setting for each climatic zone. Optimal design solutions are then derived from the combination of SVM and NSGA-II, and their sensitivities to miscellaneous weather parameters are discussed in detail.

2.1.Weather conditions of major climatic zones in China

The broad area of mainland China can be divided to five major climatic zones, namely the severe cold, cold, temperate, hot summer cold winter, and hot summer warm winter, according to GB 50176-93 (as shown in Fig.2) [25]. The fives zones are classified based on the average temperature of the coldest and hottest month, where daily temperatures under 5 ℃ or over 25 ℃ are counted towards the classification standard [26]. Harbin, Beijing, Shanghai, Kunming and Hong Kong are chosen to represent respective zone climatic characteristics with a simultaneous consideration of their population densities for which the prototype high-rise residential building can be suitable.

As suggested by existing studies [27, 28], passive building designs are closely related to main outdoor environmental parameters including the air temperature, humidity, solar radiation, wind direction and speed. These parameters vary in a large range from Hong Kong (22.33 Nº, 114.17 Eº) in the southeast corner to Harbin (47.4 Nº, 123.9 Wº) in the northeast corner as compared in Fig 3. Monthly mean temperatures generally drop from south to north with increasing local latitudes, while only Kunming (KM) in the temperate zone shows a smaller temperature difference between summer

and winter. Hong Kong (HK) and Shanghai (SH) feature high relative humidity throughout a typical year, while the other three cities are characterized by conspicuous dry and wet seasons. Beijing (BJ) and Harbin (HB) in high latitudes show higher solar radiation in summer and a tremendous drop in winter due to decreased daylight hours. However, solar radiation in KM is outstanding from Jan to April due to a higher frequency of sunny days compared to other areas. Wind velocities fluctuate around the same level in HK, HB and SH, while BJ and KM show lower wind speed in the second half of a typical year. Wind directions are broadly distributed among the five cities, where HK shows a dominating east wind and KM & BJ are dominated by north wind. These variations in the thermal, solar and wind environment can highly impact the preference over specific passive designs to maximize the benefit of natural ventilation and heat insulation. The weather data of HK are in the International Weather for Energy Calculations (IWEC) format developed from the City University of Hong Kong, while data of other cities in mainland China are derived from the Chinese Standard Weather Data (CSWD).

2.2.Building modelling and control algorithm design

As detailed in a previous study conducted by the authors [8], a generic building model (See Fig. 4) is developed in EnergyPlus to represent a typical high-rise residential building format for densely populated large cities. The generic model is assumed to operate with a setting of internal load conditions and equipment schedules based on BEAM and ASHRAE guidelines [3, 29, 30]. It has also been validated in naturally ventilated unoccupied conditions by a full-scale building measurement, where the indoor thermal, ventilation and daylight indicators showed consistent trends with simulation results [31-33].

Passive design parameters, including the building orientation (BO), external obstruction angle (EOA), wall thermal resistance (WTR), wall specific heat (WSH), window U-value (WU), solar heat gain coefficient (SHGC), overhang projection fraction (OPF), window to ground ratio (WGR) and infiltration air mass flowrate coefficient (IAMFC) are chosen model inputs distributed uniformly in specified ranges based on existing literatures and building design guidelines. The visible light transmittance (VLT) covariates with SHGC to simulate a traditional low-e glazing, while EOA is further decoupled into elementary factors of the external obstruction height (EOH) and external

obstruction distance (EOD).

The total building demands including the lighting, cooling and heating are calculated according to the lighting dimming and dynamic hybrid ventilation control specified in Fig. 4 [34]. The cooperation of the airflow network (AFN) module and HVAC systems are designed to explore the maximum energy saving potential by passive measures. The controller operates with each timestep and can override any local controls of HVAC and AFN by closing window/door openings or shutting down ventilation/mixing and activating the HVAC system under below conditions [35]. The indoor operative temperature is dynamically compared with upper and lower limits of the selected adaptive comfort model (ACM). Once the indoor operative temperature is in the comfort zone, the natural ventilation will be executed whenever the outdoor temperature is lower. Otherwise the window should be closed and the HVAC system should be operated based on the availability status of cooling or heating systems. With the above control algorithm, complying with thermal comfort criteria naturally leads to reducing HVAC loads, offering a potential solution to the contradiction between energy and comfort objectives in optimization studies [36, 37].

2.3.Sensitivity analysis approach

2.3.1. Relative weight analysis

The relative weight analysis can decompose R^2 of a multiple linear regression model as calculated by Eq. (1) to (3) into pseudo-orthogonal portions. The multiple linear regression is a simple sensitivity analysis (SA) method requiring a small sampling size of 100 per regression coefficient [38]. The relative weight is defined as the contribution of each predictor to the explainable variation in the output [39]. This indicator is derived from sequential sums of squares to avoid potential correlations between predictors. It can be used to replace the traditional partial regression coefficient. The whole calculation process is conduct by the “relweights” function in R environment.

$$\hat{y}_i = \beta_0 + \sum_{j=1}^{k} \beta_j x_j \tag{1}$$

$$\sum_{i=1}^{N} (y_i - \hat{y}_i)^2 = \sum_{i=1}^{N} \left[y_i - \left(\beta_0 + \sum_{j=1}^{k} \beta_j x_{ij} \right) \right]^2 \tag{2}$$

$$R^2 = \frac{\sum_{i=1}^{N}(\hat{y}_i - \bar{y})^2}{\sum_{i=1}^{N}(y_i - \bar{y})^2} \tag{3}$$

where x_i is the input/predictor; y_i is the output/response; $\hat{y}_i$ is the predicted y_i by the model; $\bar{y}$ is the averaged output value; and β_j is the regression coefficient deduced from the least squares method by minimizing Eq. (7).

2.3.2. FAST analysis

FAST (Fourier amplitude sensitivity test) is a widely used variance-based SA method to determine the relative importance of different model inputs. It is not limited by the model format and thus suitable for either non-linear or non-additive models, whose total output variance $V(Y)$ is decomposed as Eq. (4):

$$V(Y) = \sum_{i=1}^{k} V_i + \sum_{j>i}^{k} V_{ij} \cdots + V_{12\cdots k} \tag{4}$$

where $\sum_{i}^{k} V_i$ is the sum of conditional variances for the main effect of each input parameter; $\sum_{j>i}^{k} V_{ij}$ includes all conditional variances for interactions between two input parameters; and $V_{12\cdots k}$ stands for the conditional variance for the interaction of all inputs.

The relationship between different orders of sensitivity indices can be expressed by:

$$1 = \sum_{i=1}^{k} S_i + \sum_{j>i}^{k} S_{ij} + \cdots + S_{12\cdots k} \tag{5}$$

where the S_i is the first-order sensitivity index, which stands for the independent impact of changing one input on the output variance; S_{ij} is the second-order sensitivity index, standing for the interaction effect between inputs which cannot be explained by the superposition of S_i and S_j; $S_{12\cdots k}$ stands for the higher-order index, which is a fraction of output variance unexplainable by the summary of all lower order indices [40]. The total sensitivity index summarizing the all orders of sensitivity indices is then expressed by Eq. (6).

$$S_{Ti} = S_i + \sum_{j\neq i}^{k} S_{ij} + \cdots + S_{i\cdots j\cdots k} \tag{6}$$

Given the fact that FAST has been successfully applied in a previous SA study to provide a robust interpret of the relative importance of selected passive design strategies [30], it is used as a reference to estimate the validity of the relative weight analysis. In R environment, the "sensitivity package" is used to conduct the FAST analysis with fast99 function, where the sampling size is determined as 5610, the number of harmonics is set as 4 and the highest frequency of input factors is set as 69.

2.3.3. Application of bootstrapping

Bootstrapping is mainly used to evaluate the accuracy of SA indices from FAST, because the least-squares linear regression conducted by the "relweights" function can automatically obtain the uncertainty of regression coefficients [41]. The Plug-in principle, where the original probability distribution function F ($\theta = t(F)$) of a sensitivity index θ is replaced by the same empirical distribution function $\hat{F}$ ($\hat{\theta} = t(\hat{F})$) of a corresponding $\hat{\theta}$, is applied in a bootstrapping process [42]. It starts with creating an original dataset by modelling experiments as per section 2.3.2. Then, a bootstrap sample Z^*_1 with the exact same dimension is generated by 5610 times of resampling conducted with the package 'boot" in R environment. This process is repeated 1000 times, which are proved to be adequate for acquiring stable confidence levels of SA indices as suggested by a previous study [38]. Subsequently, the sensitivity index $\hat{\theta}^*$ is calculated for each bootstrap replication, and its standard deviation is estimated by Eq. (7) [43]:

$$S\hat{\theta}^{*} = \sqrt{\frac{1}{B-1}\sum_{k=1}^{B}(\theta_k^* - \frac{1}{B}\sum_{k=1}^{B}\theta_k^*)^2} \quad (7)$$

2.4.Surrogate model based parametric and design optimization

SVM (Support Vector Machine) is chosen for developing surrogate models in this research as suggested by a comparative study of different model fitting methods [8]. The "ksvm" function in R environment is used for conducting SVM regressions and the input type "rbfdot" is selected for the Gaussian kernel function. To evaluate the performance of developed surrogate models, R^2 defined by Eq. (3) and the Root Mean Square Error (RMSE) as per Eq. (8) are used as optimization objectives in a tuning process conducted with the "tuneParams" function in the "mlr" package of R.

$$RMSE = \sqrt{\frac{\sum_{i=1}^{N}\left(y_i - \hat{y}_i\right)^2}{N}} \quad (8)$$

Optimal SVMs from the above tuning process are further coupled with the optimization function "nsga2" in R to obtain the best design solutions under different weather conditions. "nsga2" adopts the non-dominated sorting genetic algorithm-II (NSGA-II), whose original three objectives (i.e. lighting, cooling and heating) are reduced to a single objective (i.e. the total energy demand) by summing them up with equally assigned weights (i.e. the weighted sum method) [44]. Optimization settings, including the population size, number of generations, crossover and mutation probability as well as tournament size are summarized in Table 1, according to a statistical summary of existing literatures and an adaptive variation of optimization configurations [45-47].

3. Results and discussions

This research examined the sensitivity of a proposed passive design optimization approach to a diverse variation of climatic conditions in China. The relative weight analysis method is compared with the FAST method in interpreting the relative importance of architectural design inputs for the representative city in each climatic zone. The parametric setting of SVM is also tuned in R environment to derive optimized surrogate models to further couple with NSGA-II, by which optimal passive design solutions for each weather condition are analyzed and discussed. Main results and discussions are presented in this session.

3.1.Sensitivity analysis result for different climatic zones

The relative weight analysis is first applied to the multiple linear regression model (MLR) for the building energy demand in Hong Kong. The model fitting performance is not ideal ($R^2 < 0.7$) with R^2 of 0.638 and RMSE of 5.387 kWh/m^2, which cannot adequately explain the variation in the output [8]. However, the model interpretation instead of prediction accuracy is the major concern in this analysis. Accordingly, the relative importance of each input is calculated based on MLR, where the solar heat gain coefficient (i.e. SHGC) is determined to be the most important contributor accounting for 71.4% of the explainable output variation. External and local shading factors including EOD, EOH and OPF altogether contributed to 21.6% of R^2 portions. The window thermal property (i.e. WU)

and size (i.e. WGR) are ranked after the above four inputs and contribute to 2.8% and 2.5% of R^2 portions respectively. The rest design factors are considered relatively less important with individual contributions less than 1%. In contrast, based on FAST first-order indices, SHGC is still ranked first but with a slightly smaller contribution of 68.0% to the explainable output variation. WGR and the building orientation (BO) are identified as the second and third important inputs with a contribution to R^2 portions of 10.9% and 9.1% respectively. EOD, OPF, WU and EOH are however less important inputs with a total contribution of 10.4%. In addition, WTR also has a relative contribution of 1.5% based on FAST. The above comparison of two sensitivity analysis approaches applied in HK is presented in Fig. 5.

Apart from the relative importance of design inputs derived from above analyses, FAST total-order indices were also calculated to perform factor fixing where insignificant inputs can be excluded from the optimization problem space (See Table 2). FAST total-order indices from the original dataset indicate that all input factors have either independent or interactive contributions with non-zero values, whereas an average standard error of 0.019 enabled possible zeros for the infiltration coefficient (i.e. IAMFC) and wall thermal specific heat (i.e. WSH) as illustrated by their 95% confidence intervals. As a result, IAMFC and WSH are deemed as non-influential factors which can be fixed at any possible values without major impact on the building energy demand.

When the relative weight analysis is applied to modelling experiments in KM, The MLR model also shows unacceptable R^2 of 0.468 and RMSE of 2.485 kWh/m^2, indicating a poor correlation between model inputs and outputs and the existence of non-linearity in the building model. Fig. 6 presents the comparison of SA indices from the two approaches for the building energy demand in KM. SHGC, EOD, WU, WTR and EOH are determined to be the top five influential factors as suggested by their relative weight indices. Altogether they contribute to about 95.4% of the explainable output variation. FAST first-order indices also identified the importance of the above five factors, while their ranks are slightly different. WGR is also considered an influential contributor to R^2 portions, where 9.0% and 3.1% are determined from the two methods respectively. Compared with the weighting of design inputs for HK, SHGC still ranks first in the relative importance but with less advantage over other design factors such as EOD and EOH. This results from the lower solar radiation level during the cooling period in KM as shown in Fig. 3. The influence from OPF and BO is also

weakened in KM for the same reason causing the change in SHGC. However, the thermal transfer property of windows and walls (i.e. WU and WTR) becomes more important in KM because of the lower outdoor air temperature in non-cooling periods. FAST total-order indices and their bootstrapped uncertainties are then summarized in Table 3, where BO, IAMFC and WSH are all identified as non-significant design inputs based on their confidence intervals.

In terms of applying the relative weight analysis to SH, the MLR model for the total energy demand also shows poor prediction performance with R^2 of 0.434 and RSME of 5.567 kWh/m^2. The performance of linear regression is even worse than those for previous two areas. This implies that a large part of variation in the total building energy demand cannot not be sufficiently explained by MLR. Compared with FAST first-order indices as shown in Fig. 7, SHGC makes apparently higher contribution to the variation of output, while WU shows an opposite change in its contribution. SHGC, WTR, WGR and WU are the four most important factors accounting for over 80% of R^2 portions in both approaches. BO is also considered an important design input with a relative weight index of 8.9% compared to its FAST first-order counterpart of 1.4%. Compared with KM and HK, thermal insulation (i.e. WTR) becomes more important as the winter outdoor temperature drops with the higher latitude in SH. Accompanied by the rising importance of WU and WTR, EOH and EOD contribute less to the variation of total energy demands. IAMFC and WSH are still identified as insignificant input factors due to possible zero FAST total-order indices as shown in Table 4.

The relative weight analysis is then applied to BJ and obtained relative importance indices are compared with those from FAST in Fig. 8. The MLR model for the total energy demand achieved better performance with R^2 of 0.716 and RMSE of 5.60 kWh/m^2. As illustrated in Fig. 8, both FAST first-order indices and relative weight indices show similar ranking and relative contribution to the explainable output variation. Compared with SH, the relative importance of WU continues to increase and ranks first in all design inputs accounting for about 60% of total R^2 portions. WTR and SHGC's SA indices are decreased to a small extent while still ranked second and third among all design inputs. The remaining inputs all together only accounts for about 10% of the output variation. The above change in SA indices mainly results from the decreasing outdoor temperature and radiation level in winter when the heating load becomes dominant in cold areas. In addition to IAMFC and WSH, BO and OPF are also identified not important for the total energy demand as indicated by the confidence

intervals in Table 5.

Finally, the relative weight analysis is applied to HB, where the fitted MLR model can better explain the variation in the total energy demand with R^2 of 0.807. Obtained relative weight indices and FAST first-order indices are highly consistent in terms of their contributions to the output variation (See Fig. 9). In contrast with SA indices for BJ, the relative importance of both WU and WTR is further increased leading to a joint contribution of 90% R^2 portions. The rest design inputs except WGR are all excluded from future optimization problem space due to possible zero FAST total-order indices as determined by bootstrapped confidence intervals in Table 6. WGR still matters in predicting the uncertainty of the output because of its interaction effects with WTR and WU.

From a pairwise comparison of SA indices for different climatic zones, it can be clearly seen that the outdoor temperature and solar radiation can explain the most variation of relative importance between different passive design parameters. Ranking of most important parameters generally echoes with findings of an existing SA study for the corresponding climatic zones in China, except that air-tightness is not identified as an influential input in this study because of the involvement of natural ventilation in building operation strategies [26]. The relative weight analysis can achieve efficient estimations of design input sensitivities consistent with traditional FAST when R^2 of the regression model is higher than 0.7.

3.2.Tuning surrogate models for optimization

SVM was considered most suitable for developing the surrogate model to combine with NSGA-II based on a previous study conducted in Hong Kong [8]. Its prediction accuracy in the optimization process was validated in a comparative modelling experiment with reference to the original EnergyPlus model. However, SVM models with default parametric settings show a decreased R^2 of 0.859 when the proposed dynamic hybrid ventilation control strategy is used in this modelling experiment. To improve the model fitting performance, SVM models for each climatic region are subject to parametric optimizations as per Section 2.4. When Sigma and C values change between specified distribution ranges, RMSE of the derived regression model increases with decreased R^2 as shown in Fig. 10, so that optimal Sigma and C can be obtained by maximizing mean R^2 of trained SVM models. It can be clearly concluded from the heat map in Fig. 10 that the cost parameter C has

greater influence over the model prediction performance irrespective of the selected Sigma in its distribution range.

The optimized SVM model with a tuned C value of 743.655 is compared with the original SVM with a default C value of 1.000 and the correlation between simulated and predicted total energy demands is presented in Fig. 11. The prediction error of the default SVM model grows with the total energy demands, while the optimized model can provide good estimation throughout the whole range of model outputs judging from the concentration of training data points around the ideal diagonal line. The R^2 value of the prediction model increases from 0.859 to 0.992, while RMSE decreases from 3.369 to 0.814 kWh/m^2 (i.e. 1.125% of the mean predicted total energy demand), which is considered a small and acceptable error.

SVM models for the other four climates were also optimized and their performances are summarized in Table 7. From the comparison, it can be found that all tuned statistical models can achieve excellent predicting performances with R^2 higher than 0.99. Relative errors to mean predicted model outputs are also reduced to a level between 0.881% and 3.547%, which is considered feasible for engineering applications. If RMSE is transformed to NRMSE (the normalized root mean square error) according to the definition specified by Xu et al. [48], NRMSE of the five models should be between 0.549 % to 2.062 %. This is a solid improvement derived from the above tuning process compared with an existing study where NRMSE of a fitted SVM model is up to 3.5 % [49]. These SVM models can be further coupled with NSGA-II based optimizations to minimize the computation effort for efficient design optimizations in the preliminary green building development [48].

3.3.Optimum design solutions for different climatic zones

The combination of tuned surrogate models and NSGA-II is conducted in R environment to explore the optimum design solution for each climatic zone in this section. The original integrated design optimization conduced with jEPlus took between 35816 to 39179 seconds to achieve the convergence and obtain final solutions for the five representative cities, whereas the surrogate model based optimization completed the whole process within 10 seconds [8, 50]. The weighed sum method is imposed on the cooling, heating and lighting demands so that the total energy demand becomes the single objective.

The convergence progress of optimizations under different weather conditions is illustrated in Fig. 12. The total energy demand in HK converged within the 75th generation of the weighted single objective optimization with a minimum value of 54.368 kWh/m^2. It mainly consists of a lighting demand of 30.141 kWh/m^2, a cooling demand of 23.871 kWh/m^2 and a heating demand of 0.356 kWh/m^2. This optimum design solution is attributed to a low window solar transmittance (SHGC) and wall thermal resistance (WTR) while a high window to ground ratio (WGR) and window thermal transmittance (WU). The window opening is determined to be south-facing and subject to less shadings from peripheral buildings (EOA) and overhang devices (OPF). Compared with a previous design optimization for the cooling period, the window orientation in the optimum solution shifts from north to south, which has also been observed in an existing study [27]. The above optimization results together with those for other climatic zones are summarized in Table 8.

The minimized total energy demand (27.940 kWh/m^2) for the optimization in KM is obtained in the 86th generation, with a 27.604 kWh/m^2 lighting demand, 0.058 kWh/m^2 cooling demand and 0.278 kWh/m^2 heating demand. Such a minimization of total energy demands was also observed in a similar study where a passively designed building achieved zero thermal load by optimizing seven input parameters in Kunming [51]. This optimum solution is characterized by a high window solar transmittance, U-value and wall thermal resistance. A medium-size window with less external and local shadings is also the main design feature. The main difference in design preferences between HK and KM lies in SHGC, WGR and WTR. The preference of higher solar heat gain and wall insulation results from the requirement to reduce the heating load when the cooling load is not dominating in a mild climate. The window to ground ratio should be decreased properly because the operation of natural ventilation is also reduced.

The optimum solution for SH is reached in the 74th generation with a minimum total energy demand of 48.518 kWh/m^2, decomposed to a lighting demand of 29.683 kWh/m^2, a cooling demand of 18.282 kWh/m^2 and a heating demand of 0.552 kWh/m^2. The optimized total thermal load is slightly lower than the 23.7 kWh/m^2 acquired in another passive design optimization study based on a constant HVAC set point temperature of 18 ℃ [51]. This reduction is mainly derived from the lower acceptable indoor temperature limits which are closely correlated to instantaneous outdoor temperature. The optimum design here features a reduced window U-value and window to ground

ratio compared to the scenario in HK. The change can also be attributed to the increased heating load in the cold winter. However, the wall thermal resistance of the optimum solution in SH is much lower than that in KM, resulting from the high outdoor temperature and solar radiation comparable to HK in the cooling period.

In cold and severe cold zones, the total energy demand for BJ achieved a minimum value of 27.401 kWh/m^2 within the 44th generation. It can be attributed to a lighting demand of 27.348 kWh/m^2, cooling demand of 0.048 kWh/m^2 and heating demand of 0.005 kWh/m^2. Compared to HK, the optimum solution is derived from a higher solar window transmittance and lower window to ground ratio. The wall thermal insulation is decreased due to the relaxed comfort limit in the adopted ACM for cold and severe cold areas. Similarly, the optimum design for HB also achieved minimum annual thermal loads, leading to a total energy demand of 27.798 kWh/m^2. The window U-value and window to ground ratio are further decreased while wall insulation is greatly increased compared to the scenario in BJ. The equivalent U-value of the external wall is calculated to be 0.239 W/m^2·K, which is an ideal well insulated condition with reference to ASHARE standards. The air-tightness of the optimum design also reached the highest available level in the heating period as illustrated in Fig. 13 (with a minimum ACH close to zero [52]). Again, the extremely low outdoor temperature and radiation level make space heating the major concern of design optimizations.

The optimal design in cold and severe cold areas achieved minimum HVAC demands by allocating suitable passive design measures given the specified internal load conditions [8]. According to benchmark requirements in referenced building design codes, the peak internal heat gain (30 W/m^2) consists of a people gain of 100 W/person, a lighting gain of 15 W/m^2 and an equipment gain of 142 W/Room as shown in Fig. 14. Taking the optimum design in Harbin as an example, total internal heat gains through the heating period add up to 65 kWh/m^2, which tremendously reduced the net heating load in Fig. 15. The minimized energy demand can also be attributed to the relaxed comfort limit instead of the constant indoor temperature setting adopted in most existing studies [26, 53]. The heating setpoint which covariates with the prevailing outdoor temperature can be as low as 11.4 ℃ based on the modelling results in Fig. 16. To further explore the influence of internal heat gains, Fig. 17 presented monthly heat flows in the optimal design for HB without internal gains. The calculated total heating demand is increased to 23.320 kWh/m^2, which is

slightly higher than that obtained in Gong et al.'s study [51]. Furthermore, if a constant infiltration rate of 0.5 ACH is imposed on the optimum design with no internal gains, the required total heating load is eventually increased to 43.885 kWh/m^2 (Refer to Fig. 18).

4. Conclusions

This research applied an integrated sensitivity and design optimization approach to five major climatic zones of China. Building modelling, incorporating dynamic controls, statistical analyses and surrogate model based optimizations were achieved with the cooperation of EnergyPlus and R. Based on the developed methodology, the comparison of two sensitivity analysis methods, tuning of surrogate models and design optimization of total energy demands were conducted for each climatic zone. Main findings are concluded as follows:

1) A dynamic hybrid ventilation control strategy was proposed to couple with selected passive design strategies to avoid using active building system to the largest extent. The indoor operative temperature of the generic building model was controlled within the upper and lower acceptable limits of proposed adaptive comfort models based on either the instantaneously updated outdoor temperature or prevailing mean outdoor temperature. The ASHARE 55 adaptive comfort model was applied to the hot summer warm winter, temperate, and hot summer cold winter areas, while a new model based on on-site measurements and surveys was proposed for cold and severe cold areas.
2) The relative weight analysis was adopted for factor prioritizing with reference to the validated FAST analysis by existing research. The relative weight analysis can only provide robust sensitivity indices when the fitted multiple linear regression model achieved higher R^2 than 0.7. The infiltration rate (IAMFC) and wall specific heat (WSH) were identified as non-significant design inputs for all five climatic zones based on the bootstrapped FAST total-order indices. In addition, the building orientation (BO) was excluded from the problem space of further optimization for KM and BJ, while the overhang projection ratio (OPF) was also excluded for BJ. Only the window U-value (WU), window to ground ratio (WGR) and wall thermal resistance (WTR) were considered as influential design inputs for HB.
3) The tuned SVM model for the total energy demand achieved R^2 higher than 0.99 for all five climatic zones. RMSE of these models were also reduced to a level between 0.308 to 3.203

kWh/m^2, equivalent to relative errors between 0.881 to 3.547 %. The cost parameter C was determined to be critical for increasing the model predicting performance rather than the inverse kernel width (i.e. Sigma). Developed surrogate models were then coupled with NSGA-II to perform high-efficient design optimizations for an early stage green building assessment.

4) Weighted mono-objective optimizations based on surrogate models all achieved quick convergence within 10 seconds. Obtained minimum total energy demands in five climatic zones were between 54.368 kWh/m^2 in hot summer warm winter areas to 27.401 kWh/m^2 in cold areas, where the impact of the relaxed indoor temperature setpoint, internal heat gain and infiltration rate on the total thermal load was also validated for optimum passive designs in cold and severe cold areas. Major changes in SHGC, WU, WTR and WGR were observed in optimal design solutions across the five climates. Low SHGC and high WGR are preferred in areas with a prevailing cooling requirement and great natural ventilation potential, while high WU and WTR are favorable when there is a large temperature difference across the building envelope. The insignificant design inputs as determined from sensitivity analyses presented random distributions in their defined ranges and were therefore less influenced by external weather conditions.

The proposed passive design optimization approach was successfully applied to diverse climatic zones in China with the incorporation of developed adaptive comfort models in existing studies. The weighting of design preference and final optimum solution is highly sensitive to local weather parameters such as the dry-bulb air temperature and solar radiation level. A convenient online design optimization tool coupled with geographic information systems will be developed in future research to facilitate the passive design in green building development and evaluation for broader areas.

Acknowledgment

The work described in this paper was supported by the Hong Kong PhD Fellowship Scheme, the Construction Industry Council of Hong Kong (1-ZVED) and the Research Institute for Sustainable Urban Development (RISUD) of The Hong Kong Polytechnic University (1-ZVDR). Appreciation is also given to the Housing Authority of the Hong Kong SAR Government as well as the Sino Green in Hong Kong Limited for supporting our research project in built environment studies.

Appendix

Appendix A: Adaptive comfort models used in this research

The ASHRAE 55 90% acceptability model was proved to be the most suitable ACM for the hot and humid climate of Hong Kong [6], where the outdoor temperature ranges between 10 and 33 ℃. However, such outdoor temperature requirements cannot be satisfied by the other four representative cities in colder climatic zones. In an earlier study conducted by Dear and Brager, the applicable mean outdoor temperature ranges from 5 to 32 ℃ [54]. This indicates that the ASHRAE 55 ACM is also applicable to Kunming, whose monthly average temperatures range between 8.9 ℃ and 20.3 ℃. In addition, existing studies have validated that the ASHRAE 55 ACM can successfully predict indoor thermal comfort in moderate climates and even in the summer of cold areas [15, 16]. Therefore, the ASHRAE 55 ACM is adopted as comfort criteria for cooling seasons (May to September) in HK, KM and SH as well as non-cooling seasons for HK and KM in this study. The upper and lower acceptability limits are calculated by Eq. (9) and (10):

$$T_{o,up90} = 0.31T_{ao} + 20.3 \quad (9)$$

$$T_{o,low90} = 0.31T_{ao} + 15.3 \quad (10)$$

where $T_{o,up90}$ is the upper limit of acceptable operative temperatures; $T_{o,low90}$ is the lower limit of acceptable operative temperatures; and T_{ao} is the prevailing mean outdoor air temperature as per ASHRAE 55-2013.

For the non-cooling season in SH and whole typical year in BJ and HB, more suitable models should be incorporated into the proposed dynamic hybrid ventilation control algorithm. Ye et al. recommended the below model for calculating the neutral indoor temperature T_n in Shanghai:

$$T_n = 0.42T_o + 15.12 \quad (11)$$

where T_o is the outdoor air temperature, and the 90% acceptability range is still defined to be ±2.5 as per the ASHREA 55 ACM [21].

To develop ACM for a broader spectrum of climates, Yan et al. correlated comfort survey data with the outdoor air temperature and acquired following regression equations for predicting the neutral indoor temperature in cold and severe cold areas such as Beijing and Harbin [18]:

$$T_n = 0.121T_o + 21.488 \quad (12)$$

$$T_n = 0.271T_o + 20.014 \quad (13)$$

The acceptable temperature range was given out by a similar study in the form of a polynomial equation:

$$Unacceptability\% = 120.6 - 10.49T_{ai} + 0.228T_{ai}^2$$

where T_{ai} is the acceptable average indoor air temperature, so that the 90% acceptability range should be ±6.5 around the neutral temperature [19, 20].

Appendix B: R packages for machine learning

SVM is a non-parametric modelling algorithm capable of the non-linear classification, regression, and outlier detection through an intuitive model representation [55]. Its advantage over other non-parametric model fitting methods has been well approved by existing literatures [56]. In a SVM regression, the Gaussian kernel function, taking the form of Eq. (14), is obtained by minimizing the deviation from the outputs of training data.

$$k(x, x') = \exp(-\sigma \| x - x^{'}) \|^2) \quad (14)$$

where σ (Sigma) is the inverse kernel width used by the Gaussian kernel.

The "mlr" package is designed to optimize parameter settings for different machine learning methods. In this study, R^2 is maximized and RMSE is minimized simultaneously to obtain the most suitable SVM model to be incorporated into the design optimization approach. Two important input factors of "ksvm", Sigma and C are presumed to vary uniformly between 10^{-1} and 10^{10} to form the search space of the tuning function. C (with a default value of 1.0) is the cost parameter penalizing large residuals, so that a larger C suggests less model constraints. A random search operation with the function "makeTuneControlRandom" is chosen as the optimization algorithm. Maximum iteration is set to 500 times and the "holdout" strategy is selected for conducting resampling by splitting the input sample set to a training and test set based on a prescribed ratio.

References

[1] Zhang Y, He C-Q, Tang B-J, Wei Y-M. China's energy consumption in the building sector: A life cycle approach. Energy and Buildings. 2015;94:240-51.
[2] Census and Statistics Department, Population by type of housing. 2016.
[3] BEAM. BEAM Plus New Buildings Version 1.2. HKGBC and BEAM Society Limited. 2012.

[4] Lee WL, Yik FWH, Burnett J. Assessing energy performance in the latest versions of Hong Kong Building Environmental Assessment Method (HK-BEAM). Energy and Buildings. 2007;39:343-54.
[5] Chen X, Yang H, Lu L. A comprehensive review on passive design approaches in green building rating tools. Renewable and Sustainable Energy Reviews. 2015;50:1425-36.
[6] Chen X, Yang H, Wang Y. Parametric study of passive design strategies for high-rise residential buildings in hot and humid climates: miscellaneous impact factors. Renewable and Sustainable Energy Reviews. 2017;69:442-60.
[7] Chen X, Yang H, Zhang W. A comprehensive sensitivity study of major passive design parameters for the public rental housing development in Hong Kong. Energy. 2015;93:1804-18.
[8] Chen X, Yang H. A multi-stage optimization of passively designed high-rise residential buildings in multiple building operation scenarios. Applied Energy. 2017;206:541-57.
[9] Luo M, Cao B, Damiens J, Lin B, Zhu Y. Evaluating thermal comfort in mixed-mode buildings: A field study in a subtropical climate. Building and Environment. 2015;88:46-54.
[10] ASHRAE. ASHRAE 55-2004: Thermal Environmental Conditions for Human Occupancy. Atlanta2004.
[11] de Dear RJ, Brager GS. Thermal comfort in naturally ventilated buildings: revisions to ASHRAE Standard 55. Energy and Buildings. 2002;34:549-61.
[12] KIBAYA LR. THERMAL COMFORT ANALYSIS OF A NATURALLY VENTILATED BUILDING: FACULTY OF ENGINEERING AND SUSTAINABLE DEVELOPMENT, UNIVERSITY OF GAVLE; 2013.
[13] Attia S, Carlucci S. Impact of different thermal comfort models on zero energy residential buildings in hot climate. Energy and Buildings. 2015;102:117-28.
[14] Sorgato MJ, Melo AP, Lamberts R. The effect of window opening ventilation control on residential building energy consumption. Energy and Buildings. 2016;133:1-13.
[15] Zhang A, Bokel R, van den Dobbelsteen A, Sun Y, Huang Q, Zhang Q. Optimization of thermal and daylight performance of school buildings based on a multi-objective genetic algorithm in the cold climate of China. Energy and Buildings. 2017;139:371-84.
[16] Ortiz J, Fonseca A, Salom J, Garrido N, Fonseca P, Russo V. Comfort and economic criteria for selecting passive measures for the energy refurbishment of residential buildings in Catalonia. Energy and Buildings. 2016;110:195-210.
[17] Desogus G, Di Benedetto S, Ricciu R. The use of adaptive thermal comfort models to evaluate the summer performance of a Mediterranean earth building. Energy and Buildings. 2015;104:350-9.
[18] Yan H, Mao Y, Yang L. Thermal adaptive models in the residential buildings in different climate zones of Eastern China. Energy and Buildings. 2017;141:28-38.
[19] Yu W, Li B, Yao R, Wang D, Li K. A study of thermal comfort in residential buildings on the Tibetan Plateau, China. Building and Environment. 2017;119:71-86.
[20] Yang L, Yan H, Xu Y, Lam JC. Residential thermal environment in cold climates at high altitudes and building energy use implications. Energy and Buildings. 2013;62:139-45.
[21] van Hoof J, Hensen JLM. Quantifying the relevance of adaptive thermal comfort models in moderate thermal climate zones. Building and Environment. 2007;42:156-70.
[22] Sourbron M, Helsen L. Evaluation of adaptive thermal comfort models in moderate climates and their impact on energy use in office buildings. Energy and Buildings. 2011;43:423-32.

[23] Barbadilla-Martín E, Salmerón Lissén JM, Guadix Martín J, Aparicio-Ruiz P, Brotas L. Field study on adaptive thermal comfort in mixed mode office buildings in southwestern area of Spain. Building and Environment. 2017;123:163-75.
[24] Bhaskoro PT, Gilani SIUH, Aris MS. Simulation of energy saving potential of a centralized HVAC system in an academic building using adaptive cooling technique. Energy Conversion and Management. 2013;75:617-28.
[25] Hong T. A close look at the China Design Standard for Energy Efficiency of Public Buildings. Energy and Buildings. 2009;41:426-35.
[26] Zhao M, Künzel HM, Antretter F. Parameters influencing the energy performance of residential buildings in different Chinese climate zones. Energy and Buildings. 2015;96:64-75.
[27] Delgarm N, Sajadi B, Kowsary F, Delgarm S. Multi-objective optimization of the building energy performance: A simulation-based approach by means of particle swarm optimization (PSO). Applied Energy. 2016;170:293-303.
[28] Kneifel J, Webb D. Predicting energy performance of a net-zero energy building: A statistical approach. Applied Energy. 2016;178:468-83.
[29] ASHRAE. 2009 ASHRAE® HANDBOOK FUNDAMENTALS. Atlanta2009.
[30] Chen X, Yang H, Wang T. Developing a robust assessment system for the passive design approach in the green building rating scheme of Hong Kong. Journal of Cleaner Production. 2017;153:176-94.
[31] Zhai Z, Johnson M-H, Krarti M. Assessment of natural and hybrid ventilation models in whole-building energy simulations. Energy and Buildings. 2011;43:2251-61.
[32] Schulze T, Eicker U. Controlled natural ventilation for energy efficient buildings. Energy and Buildings. 2013;56:221-32.
[33] Chen X, Yang H. Combined thermal and daylight analysis of a typical public rental housing development to fulfil green building guidance in Hong Kong. Energy and Buildings. 2015;108:420-32.
[34] CIBSE. Code for Lighting. Chartered Institution of Building Services Engineers, London; 2002.
[35] ENERGYPLUS™. EnergyPlus Engineering Reference - The Reference to EnergyPlus Calculations: US Department of Energy; 2013.
[36] Martinez NA. Solving the Black Box: Inverse Approach for Ideal Building Dynamic Behaviour Using Multi-Objective Optimization with Energyplus. 8th Windsor Conference: Counting the cost of comfort in a changing world. Cumberland Lodge, Windsor, UK, 10-13 April 2014. London: Network for Comfort and Energy Use in Buildings2014.
[37] Negendahl K, Nielsen TR. Building energy optimization in the early design stages: A simplified method. Energy and Buildings. 2015;105:88-99.
[38] Chen X, Yang H, Sun K. Developing a meta-model for sensitivity analyses and prediction of building performance for passively designed high-rise residential buildings. Applied Energy. 2017;194:422-39.
[39] Groemping U. Relative Importance for Linear Regression in R: The Package relaimpo. 2006. 2006;17:27.
[40] Mechri HE, Capozzoli A, Corrado V. USE of the ANOVA approach for sensitive building energy design. Applied Energy. 2010;87:3073-83.
[41] Tian W, Song J, Li Z, de Wilde P. Bootstrap techniques for sensitivity analysis and model selection in building thermal performance analysis. Applied Energy. 2014;135:320-8.

[42] Efron B, Tibshirani R. An introduction to the bootstrap: Chapman & Hall Inc.; 1993.
[43] James G, Witten D, Hastie T, Tibshirani R. An Introduction to Statistical Learning with Application in R: Springer; 2013.
[44] Deb K. Multi-objective optimization using evolutionary algorithms. 1st ed. Chichester, New York, N.Y: John Wiley & Sons; 2001.
[45] Hamdy M, Nguyen A-T, Hensen JLM. A performance comparison of multi-objective optimization algorithms for solving nearly-zero-energy-building design problems. Energy and Buildings. 2016;121:57-71.
[46] Carlucci S, Cattarin G, Causone F, Pagliano L. Multi-objective optimization of a nearly zero-energy building based on thermal and visual discomfort minimization using a non-dominated sorting genetic algorithm (NSGA-II). Energy and Buildings. 2015;104:378-94.
[47] Chen X, Yang H, Zhang W. Simulation-based approach to optimize passively designed buildings: A case study on a typical architectural form in hot and humid climates. Renewable and Sustainable Energy Reviews.
[48] Xu W, Chong A, Karaguzel OT, Lam KP. Improving evolutionary algorithm performance for integer type multi-objective building system design optimization. Energy and Buildings. 2016;127:714-29.
[49] Melo AP, Versage RS, Sawaya G, Lamberts R. A novel surrogate model to support building energy labelling system: A new approach to assess cooling energy demand in commercial buildings. Energy and Buildings. 2016;131:233-47.
[50] Chen X, Yang H, Sun K. A holistic passive design approach to optimize indoor environmental quality of a typical residential building in Hong Kong. Energy. 2016;113:267-81.
[51] Gong X, Akashi Y, Sumiyoshi D. Optimization of passive design measures for residential buildings in different Chinese areas. Building and Environment. 2012;58:46-57.
[52] Ji Y, Duanmu L. Air-tightness test and air infiltration estimation of an ultra-low energy building. Science and Technology for the Built Environment. 2017;23:441-8.
[53] van Hooff T, Blocken B, Timmermans HJP, Hensen JLM. Analysis of the predicted effect of passive climate adaptation measures on energy demand for cooling and heating in a residential building. Energy. 2016;94:811-20.
[54] de Dear R, Schiller Brager G. The adaptive model of thermal comfort and energy conservation in the built environment. International Journal of Biometeorology. 2001;45:100-8.
[55] Meyer D. Support Vector Machines - The Interface to libsvm in package e1071. FH Technikum Wien, Austria. 2017.
[56] Rackes A, Melo AP, Lamberts R. Naturally comfortable and sustainable: Informed design guidance and performance labeling for passive commercial buildings in hot climates. Applied Energy. 2016;174:256-74.

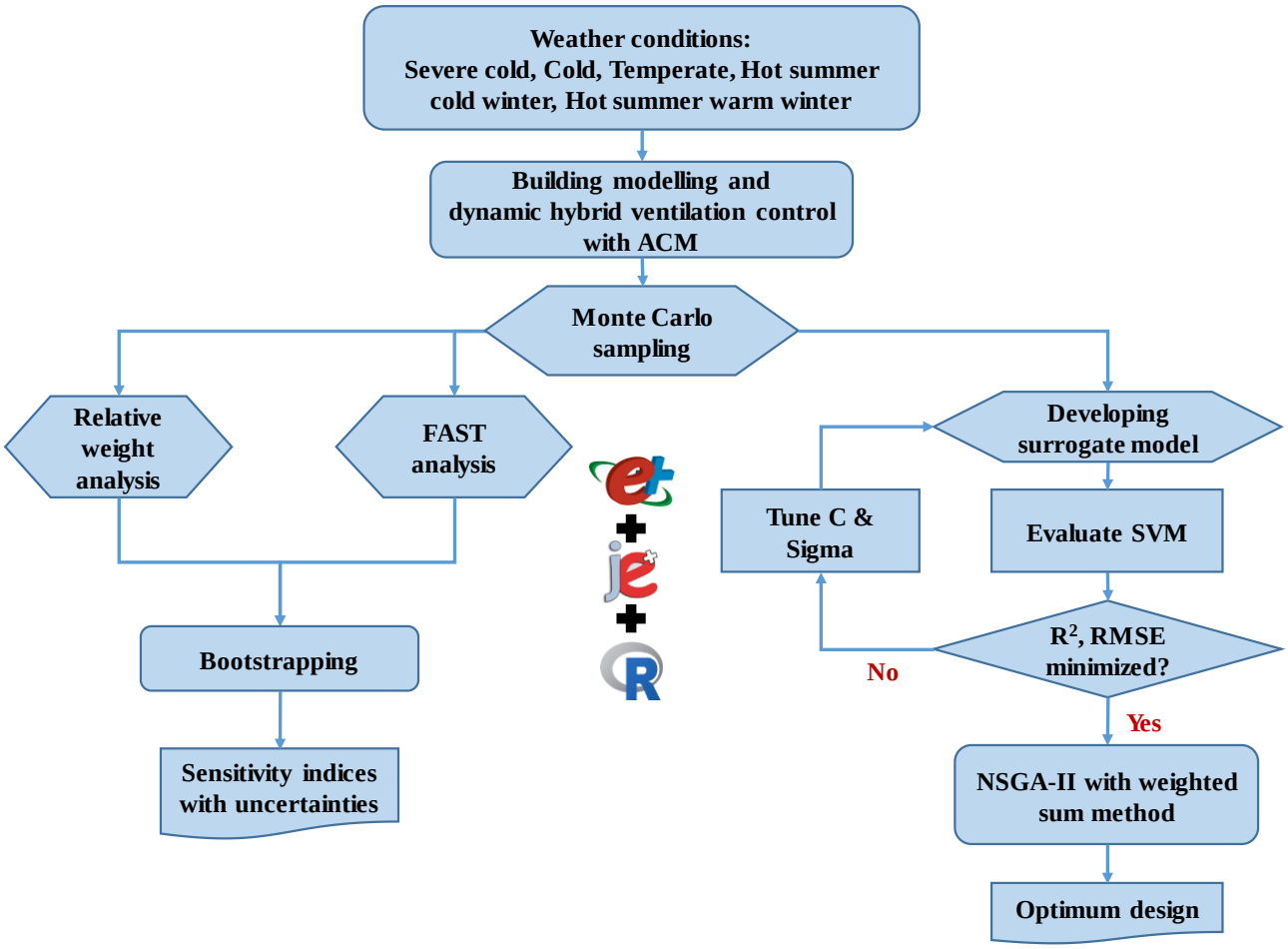

Fig. 1 Proposed research design framework

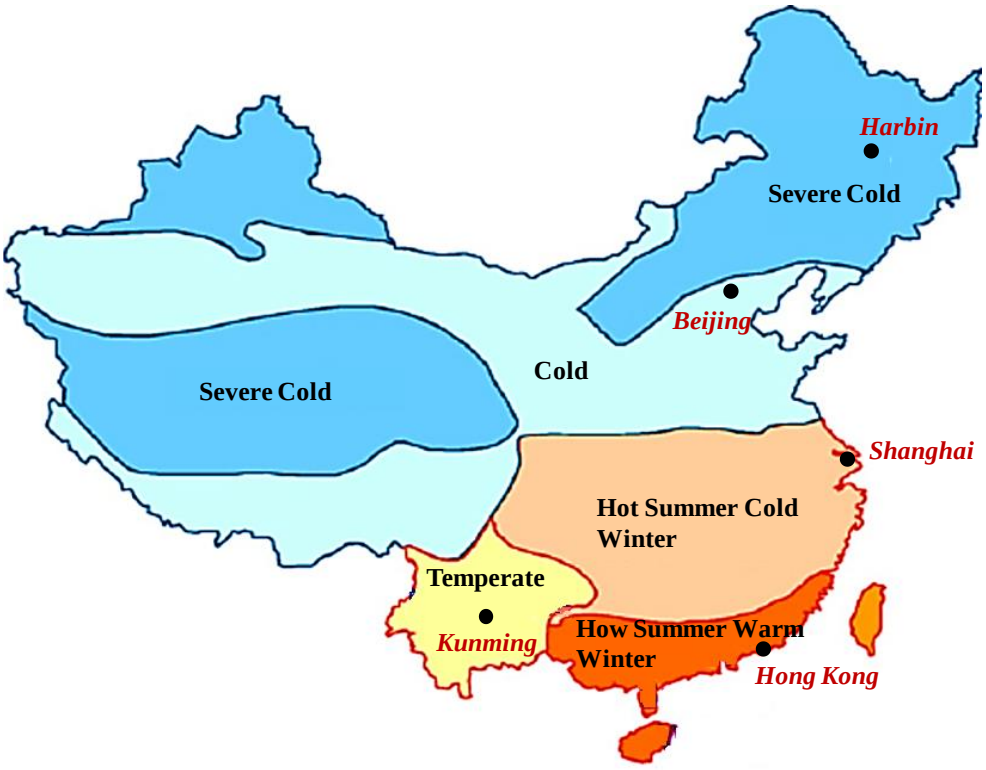

Fig. 2 Climatic zoning in China and selected representative cities

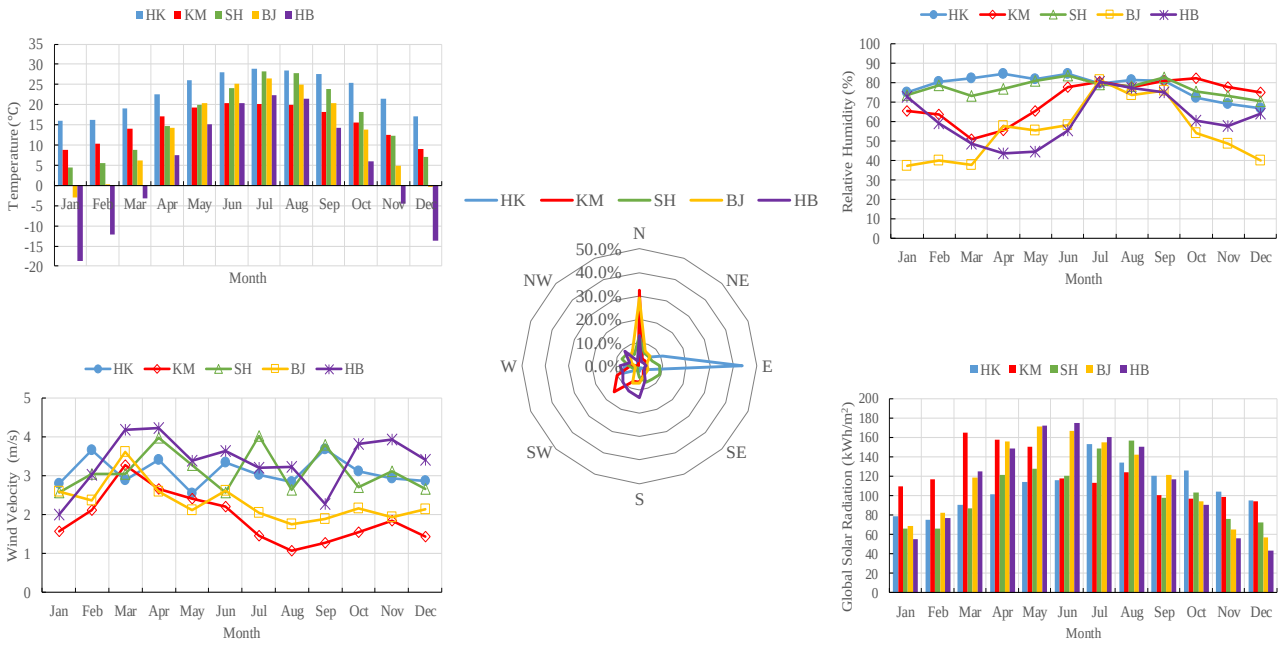

Fig. 3. Comparison of main weather parameters in the five cities

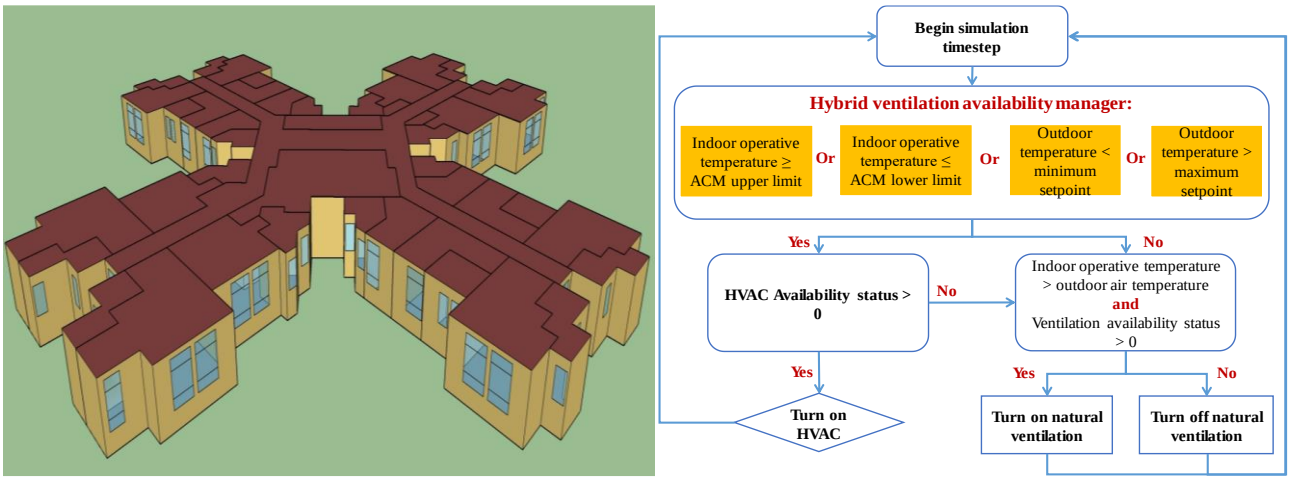

Fig. 4 The typical floor model and hybrid ventilation control algorithm

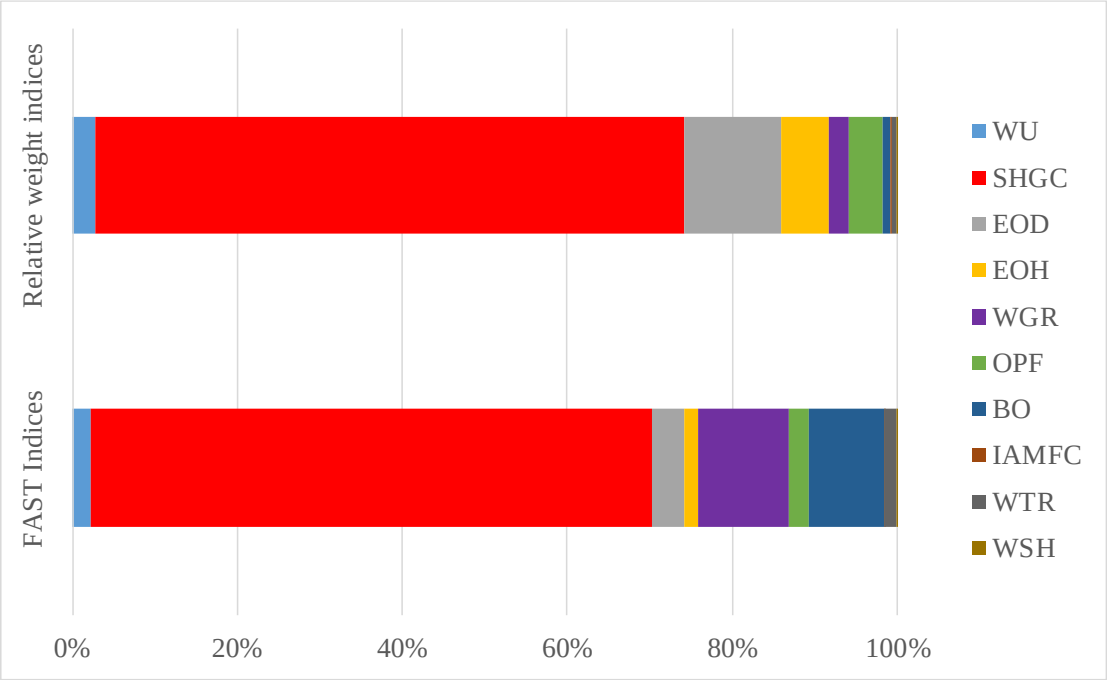

Fig. 5 Comparison of two sensitivity analysis approaches for the application in HK

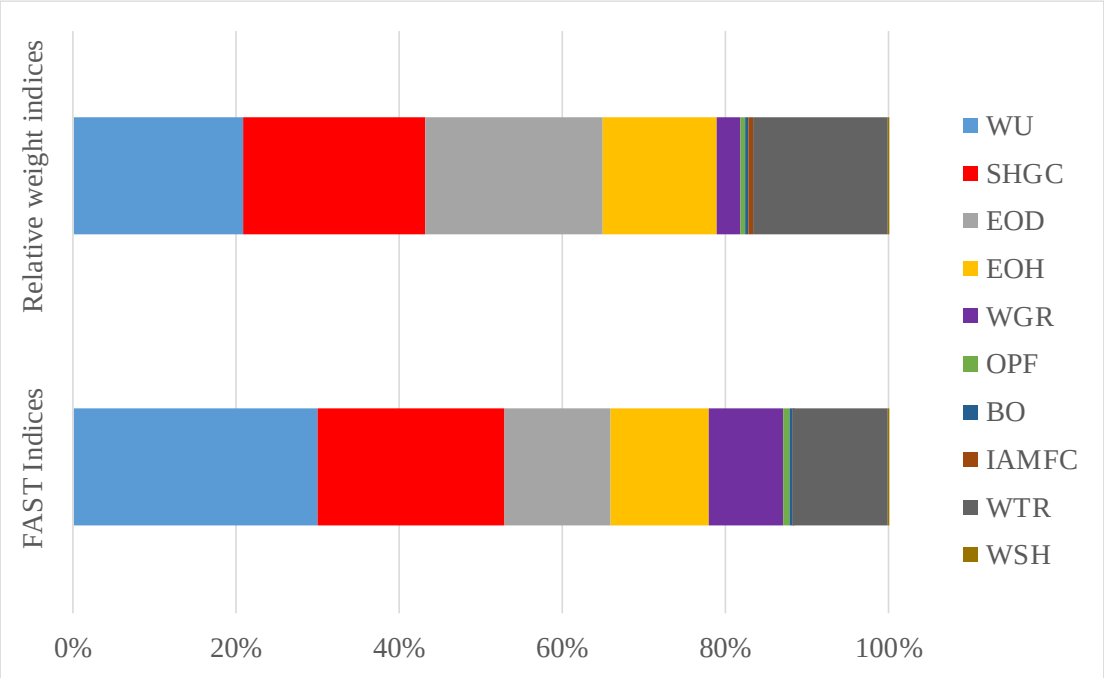

Fig. 6 Comparison of two sensitivity analysis approaches for the application in KM

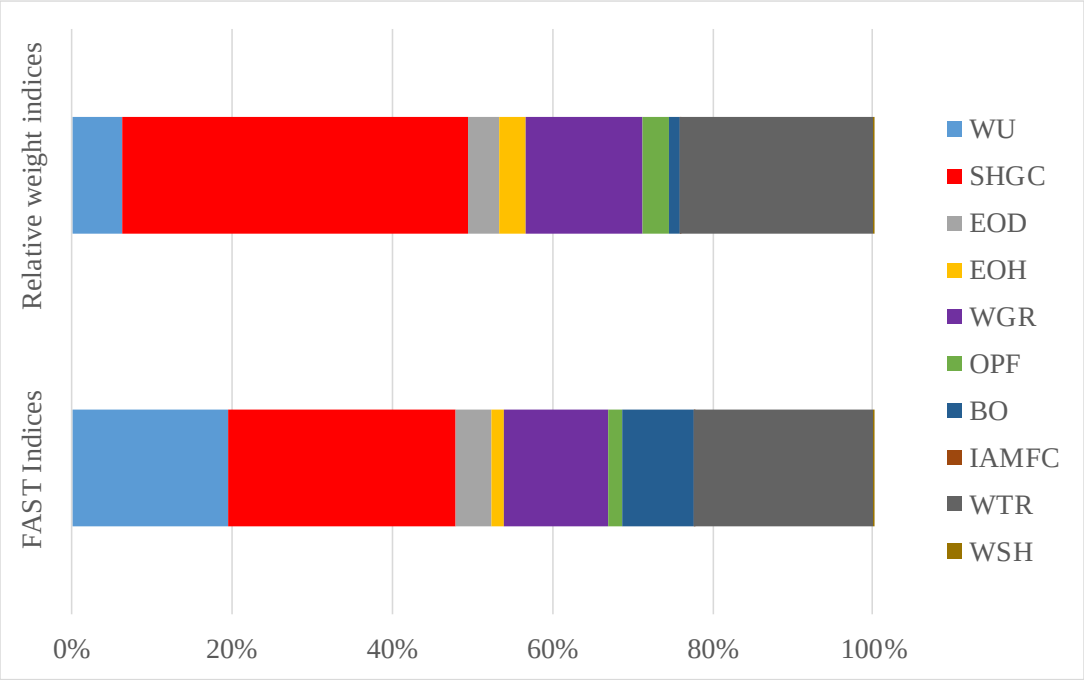

Fig. 7 Comparison of two sensitivity analysis approaches for the application in SH

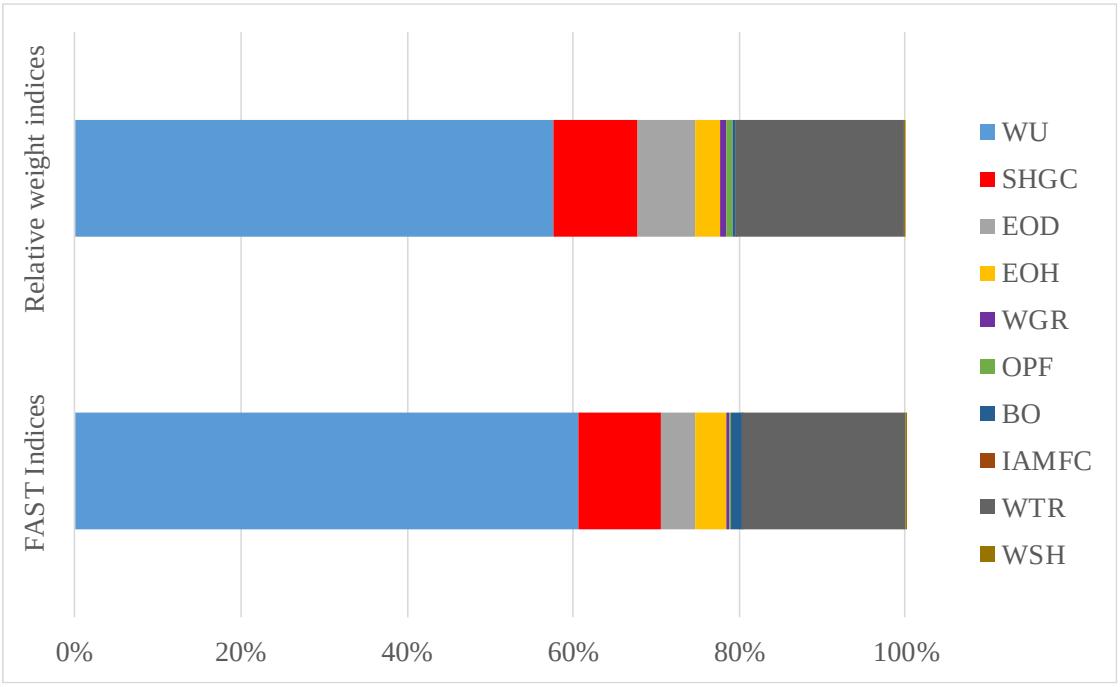

Fig. 8 Comparison of two sensitivity analysis approaches for the application in BJ

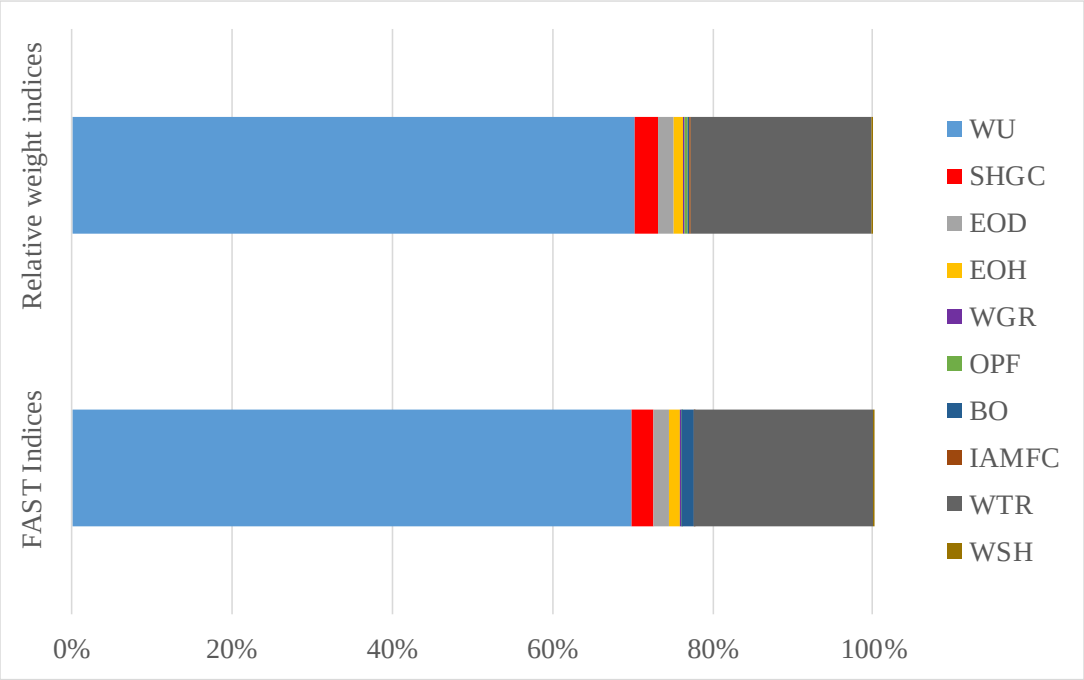

Fig. 9 Comparison of two sensitivity analysis approaches for the application in HB

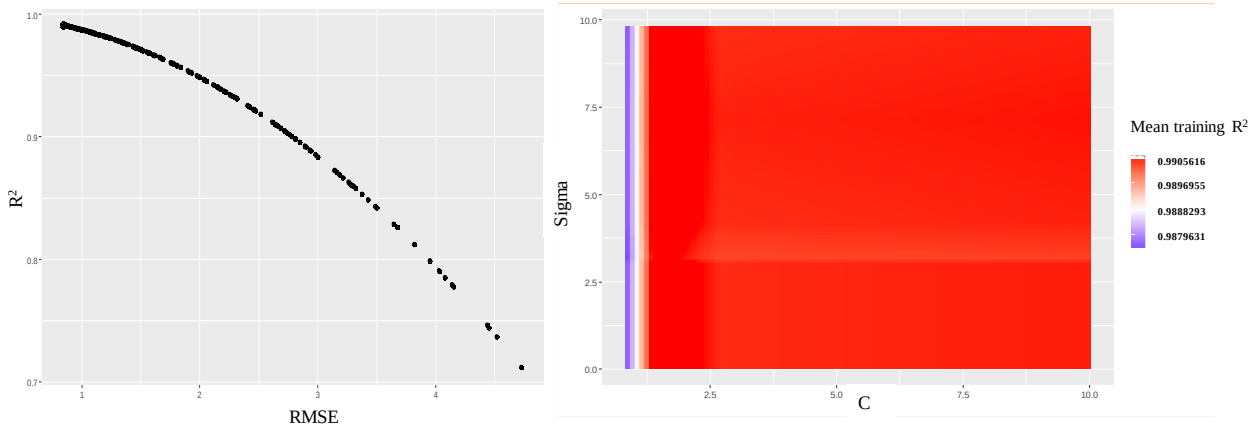

Fig. 10 Parametric optimization results for the SVM model in HK

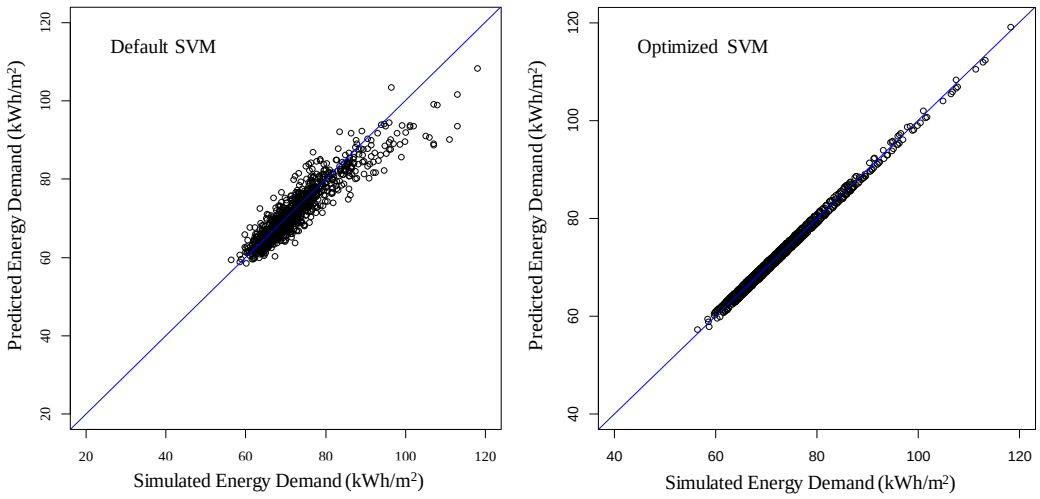

Fig. 11 Comparison of SVM model performances

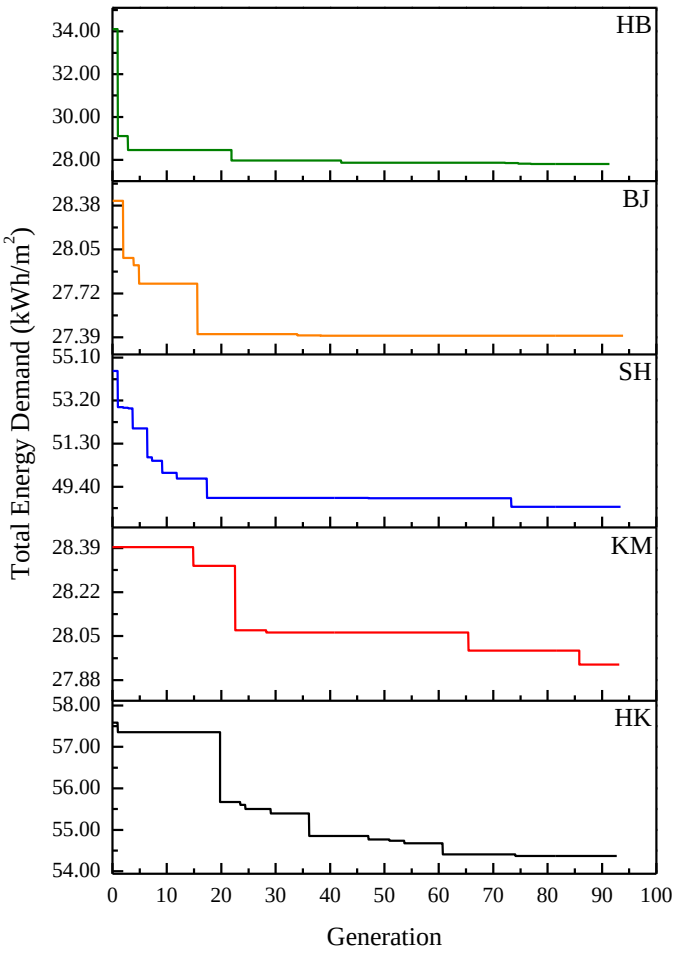

Fig. 12 Convergence progress of the optimization process for five climatic zones

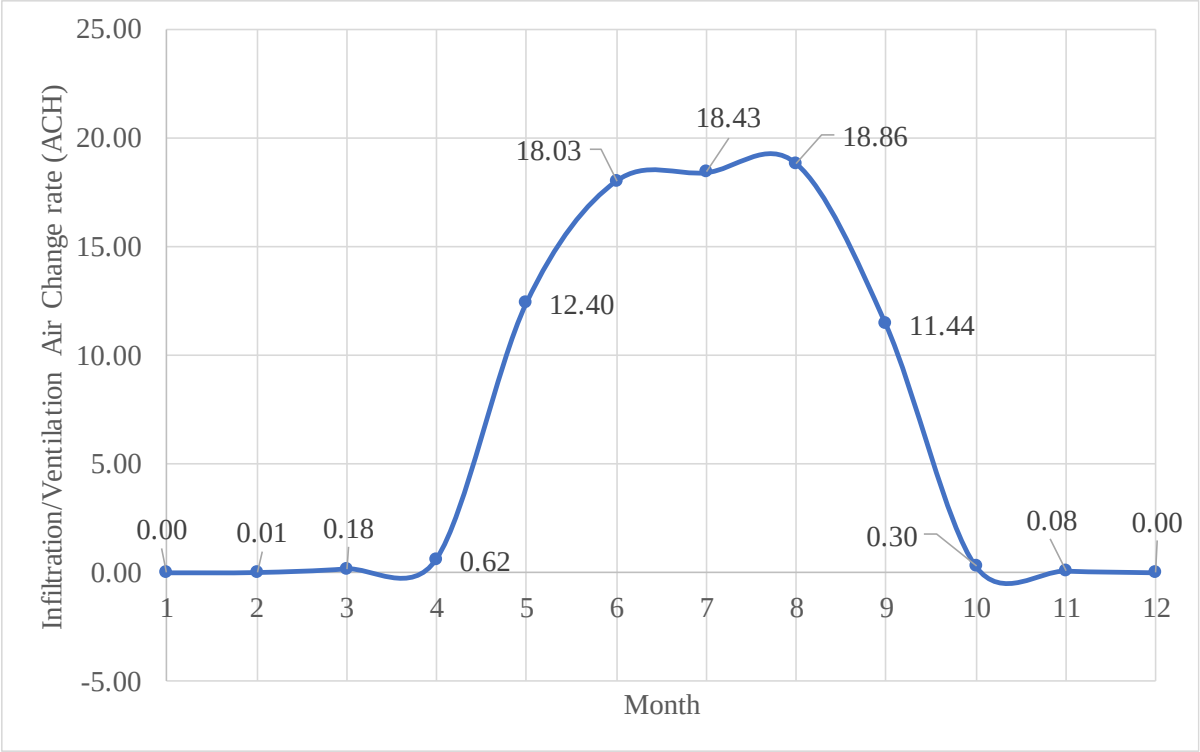

Fig. 13 The predicted monthly average ACH of the optimum design for Harbin

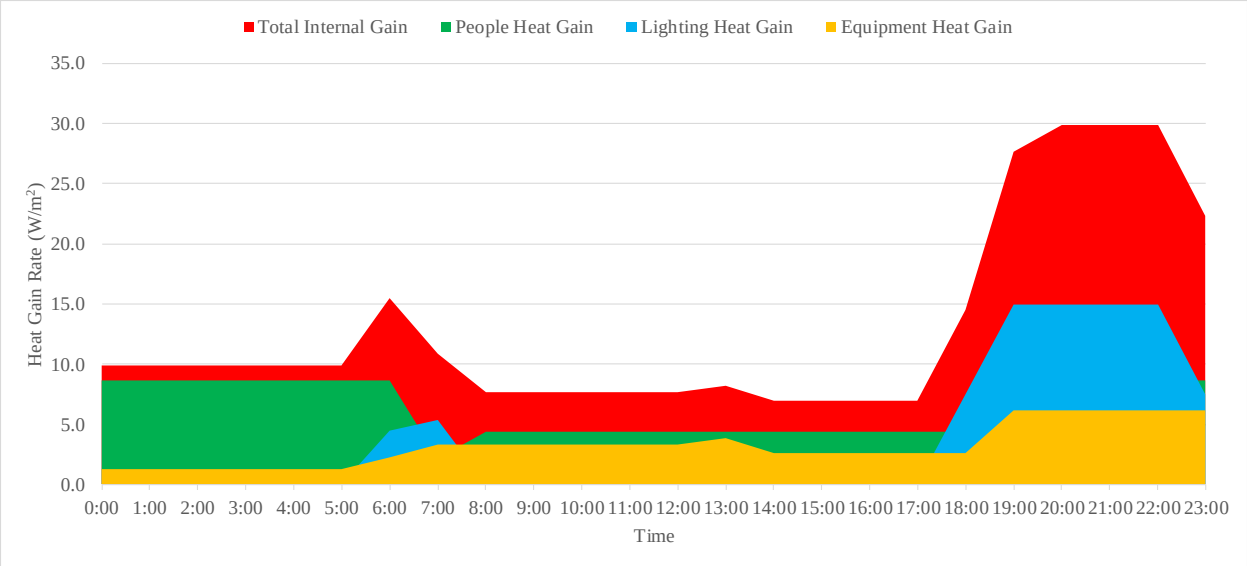

Fig. 14 Miscellaneous internal loads in a typical day of the simulation

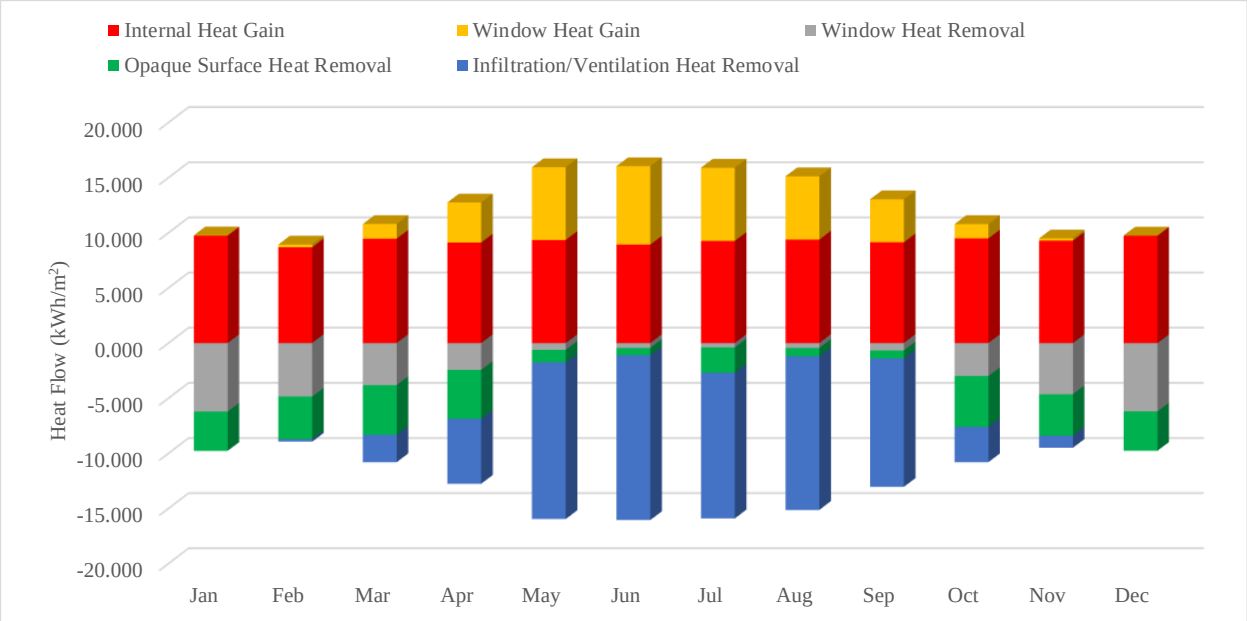

Fig. 15 Monthly heat flows of the optimum design for Harbin

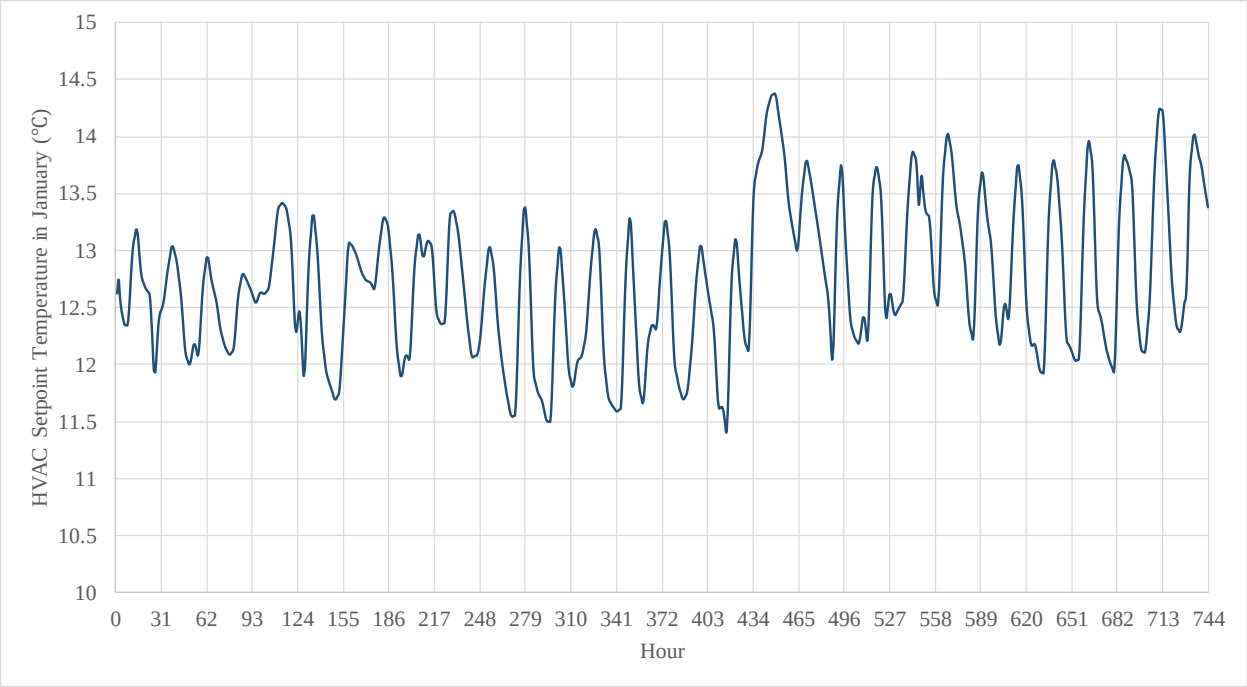

Fig. 16 HVAC setpoint temperature based on proposed adaptive comfort model for Harbin in the coldest month

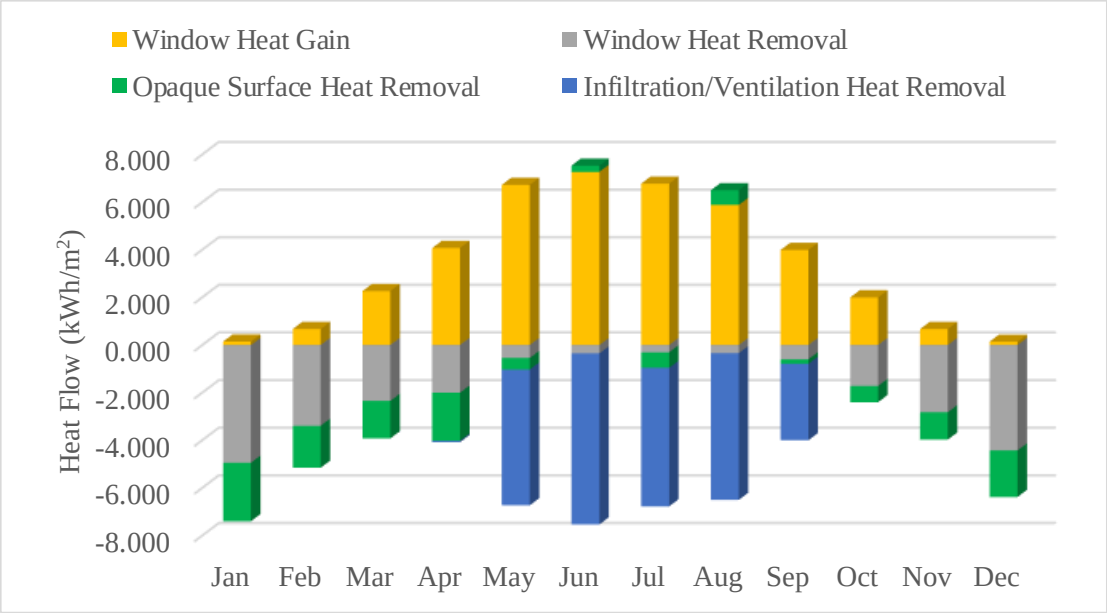

Fig. 17 Monthly heat flows of the optimum design for Harbin with no internal heat gains

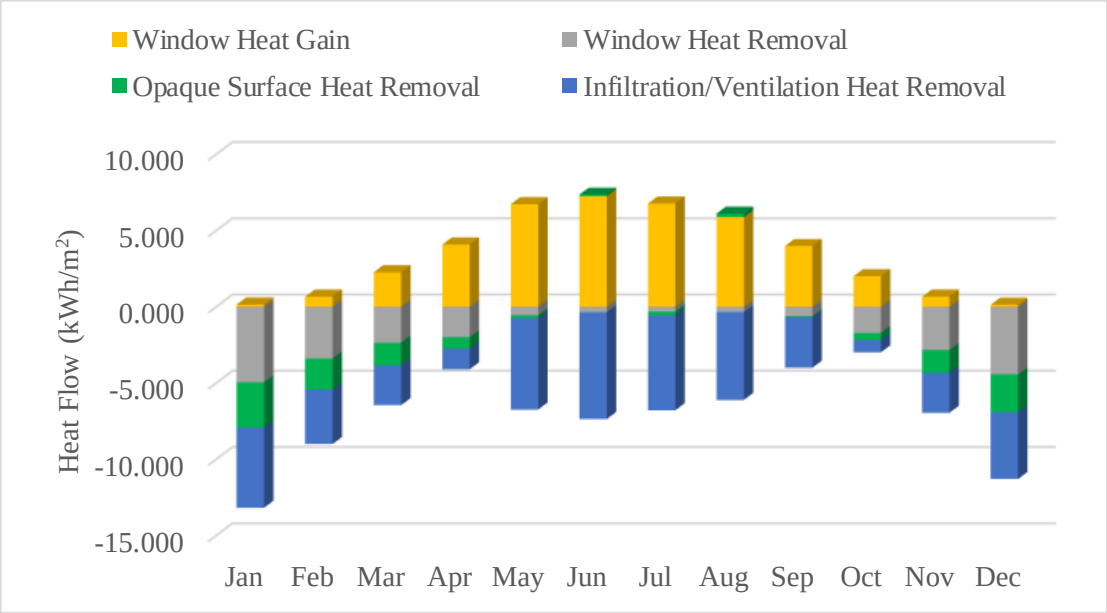

Fig. 18 Monthly heat flows of the optimum design for Harbin with no internal heat gains and increased infiltration

Table 1 Setting of the optimization algorithm

Parameter	Value
Population size	20
Number of generations	100
Crossover probability	0.9
Mutation probability	0.355
Tournament size	2

Table 2 Bootstrapped FAST total-order indices for the application in HK

	Original FAST total-order indices	Standard error	95% confidence interval lower	95% confidence interval upper
WU	0.045	0.020	0.007	0.083
SHGC	0.714	0.020	0.675	0.753
WGR	0.128	0.020	0.089	0.167
EOD	0.149	0.019	0.111	0.187
EOH	0.179	0.019	0.141	0.217
OPF	0.068	0.019	0.031	0.105
BO	0.161	0.019	0.124	0.198
IAMFC	0.030	0.019	-0.007	0.067
WTR	0.048	0.020	0.009	0.087
WSH	0.016	0.019	-0.022	0.053

Table 3 Bootstrapped FAST total-order indices for the application in KM

	Original FAST total-order indices	Standard error	95% confidence interval lower	95% confidence interval upper
WU	0.355	0.020	0.317	0.393
SHGC	0.290	0.020	0.252	0.328
WGR	0.119	0.019	0.082	0.157
EOD	0.121	0.020	0.083	0.160
EOH	0.186	0.019	0.148	0.224
OPF	0.039	0.020	0.000	0.078
BO	0.015	0.020	-0.025	0.055
IAMFC	0.016	0.019	-0.021	0.053
WTR	0.172	0.020	0.134	0.210
WSH	0.030	0.020	-0.009	0.068

Table 4 Bootstrapped FAST total-order indices for the application in SH

	Original FAST total-order indices	Standard error	95% confidence interval lower	95% confidence interval upper
WU	0.304	0.019	0.266	0.341
SHGC	0.454	0.019	0.416	0.491
WGR	0.170	0.020	0.131	0.210
EOD	0.166	0.020	0.128	0.204
EOH	0.322	0.020	0.283	0.360
OPF	0.059	0.020	0.021	0.098
BO	0.164	0.018	0.128	0.200
IAMFC	0.032	0.020	-0.007	0.071
WTR	0.316	0.019	0.278	0.353
WSH	0.016	0.020	-0.022	0.055

Table 5 Bootstrapped FAST total-order indices for the application in BJ

	Original FAST total-order indices	Standard error	95% confidence interval lower	95% confidence interval upper
WU	0.575	0.019	0.538	0.612
SHGC	0.104	0.019	0.066	0.142
WGR	0.057	0.019	0.018	0.095
EOD	0.058	0.020	0.020	0.097
EOH	0.103	0.020	0.064	0.142
OPF	0.007	0.019	-0.031	0.046
BO	0.027	0.019	-0.011	0.064
IAMFC	0.005	0.020	-0.034	0.044
WTR	0.224	0.019	0.187	0.262
WSH	0.008	0.020	-0.030	0.046

Table 6 Bootstrapped FAST total-order indices for the application in HB

	Original FAST total-order indices	Standard error	95% confidence interval lower	95% confidence interval upper
WU	0.677	0.020	0.638	0.717
SHGC	0.035	0.019	-0.003	0.073
WGR	0.038	0.020	0.000	0.076
EOD	0.030	0.019	-0.008	0.068
EOH	0.122	0.020	0.083	0.161
OPF	0.004	0.019	-0.034	0.042
BO	0.026	0.019	-0.012	0.064
IAMFC	0.004	0.019	-0.034	0.041
WTR	0.261	0.019	0.223	0.299
WSH	0.006	0.020	-0.033	0.045

Table 7 Comparison between optimized and default SVM models

		R^2	RMSE (kWh/m^2)	Relative error (%)
HK	Default SVM	0.859	3.369	4.654
	Optimized SVM	0.992	0.814	1.125
KM	Default SVM	0.833	1.396	3.986
	Optimized SVM	0.992	0.308	0.881
SH	Default SVM	0.789	3.401	5.361
	Optimized SVM	0.991	0.689	1.086
BJ	Default SVM	0.935	2.877	6.846
	Optimized SVM	0.992	0.997	2.373
HB	Default SVM	0.967	6.998	7.751
	Optimized SVM	0.993	3.203	3.547

Table 8. Comparison of optimum solutions for major climatic zones in China

	HK	KM	SH	BJ	HB
WU ($W/m^2 \cdot K$)	4.590*	5.970*	3.206*	4.399*	1.777*
SHGC/VLT (-)	0.105*	0.745*	0.139*	0.852*	0.786
EOA (°)	10.007*	13.943*	5.532*	6.282*	7.527
WGR (-)	0.434*	0.217*	0.273*	0.328*	0.172*
OPF (-)	0.122*	0.056*	0.094*	0.102	0.083
BO (°)	158*	162	165*	193	328
IAMFC (kg/s)	0.025	0.021	0.020	0.026	0.011
WTR ($m^2 \cdot K/W$)	0.687*	7.647*	0.916*	0.318*	4.025*
WSH ($J/kg \cdot K$)	1713	1033	921	1121	906
Lighting energy demand (kWh/m^2)	30.141	27.604	29.683	27.348	27.795
Cooling energy demand (kWh/m^2)	23.872	0.058	18.282	0.048	0.000
Heating energy demand (kWh/m^2)	0.356	0.278	0.552	0.005	0.000
Total energy demand (kWh/m^2)	54.368	27.940	48.518	27.401	27.798
Note: * stands for significant design inputs for the total energy demand.					